



Substrate polarization effects on the plasmon excitations of small Na atomic chains on Si surfacesJ. Chen ¹, L. Q. Lai,¹ J. Quan,² Q. H. Liu,¹ and Y. B. Yu ^{1,*}¹*School of Physics and Electronics, Hunan University, Changsha 410082, China*²*School of Physical Science and Technology, Lingnan Normal University, Zhanjiang 524048, China*

(Received 22 December 2020; revised 21 February 2021; accepted 3 March 2021; published 16 March 2021)

The plasmon excitations in small metal-atom clusters have been extensively investigated in recent years, and most of the efforts are focused on freestanding clusters. However, freestanding clusters are inherently unstable and have to be stabilized by interacting with a two-dimensional or three-dimensional substrate; hence, the effects of substrates should be taken into account in the calculations of electronic excitations. With the use of the random-phase approximation, we extensively investigate the polarization effects of substrates on the plasmon resonances of small Na chains on Si surfaces. Our results show that due to the polarization effects of Si substrates, the redshifts of plasmon peaks appear in both longitudinal and transverse absorption spectra, and the strengths of the main plasmon resonant peaks have some variation; in particular, the strength gets a very large enhancement when the external field is applied in the direction perpendicular to the surface of Si. In addition, we study the formation mechanism of the end mode and the central mode of transverse-plasmon excitations and show that the two modes are caused by electron-electron interactions, which reflects the collective excitations induced by the interactions.

DOI: [10.1103/PhysRevB.103.125417](https://doi.org/10.1103/PhysRevB.103.125417)**I. INTRODUCTION**

In the last few decades, the plasmon excitations in nanostructures of metal materials have been extensively investigated due to their unique properties, such as negative-refraction phenomena [1–3], local- and near-field enhancement [4,5], photochemical reactions [6,7], nonlinear-optical responses [8,9], etc. One example of such a class of metal structures is small atomic chains which would be the ideal choice for directed energy transport in the development of electronic devices and other functional applications [10,11]. The metal atomic chains can be artificially fabricated or self-assembled [12–18], and they are supported on substrates. Since freestanding atomic chains are inherently unstable and have to be stabilized by interacting with a two-dimensional or three-dimensional substrate, whether the substrates affect the corresponding plasmon excitations needs to be considered in the calculations of electronic and structural properties for metal atomic chains. Tsukada *et al.* [19] explained that as a semi-infinite dielectric medium the semiconducting substrate has a polarization effect on the dispersion relations of surface plasmons of a parallel-rod model. Ishida *et al.* [20] employed the same method to calculate the dispersion relations of an interband plasmon model on the Si(100)(2×1)-K surface and found that K 4s-like and K 4p_x-like bands reproduced the features of observed plasmon dispersion. For noble metals, Lichtenstein *et al.* [21] recently reported the properties of one-dimensional (1D) Au chains on stepped Si(557) and demonstrated that the substrate effects can be described by the dielectric function of Si, which caused the calculated curves of the plasmon dispersion to be in very good

agreement with the experimental data. Moudgil *et al.* [22] theoretically proved that the dielectric function of Si can be used to represent the effects of the substrates in Si(557)-Au systems. In addition, if Au atomic chains ride on Si(335) or Si(775), the semiconducting substrates will have greater influence on the excitation properties of plasmons. The plasmon dispersion of Si(335)-Au and Si(775)-Au systems using the density functional theory (DFT) gives a satisfactory result that fits the measured data [16]. These examples show that the plasmon excitations of metal atomic chains are affected by interacting with Si substrates. However, in the literature about the plasmon excitations of metal atomic chains, we find that the main research objectives are devoted to freestanding atomic chains [23–41] and are rarely about the atomic chains supported on substrates [42–46]. Motivated by these points, we systematically investigate the polarization effects of Si substrates on plasmon excitations of small Na chains.

In this paper, the small atomic chains are mimicked by a model of a quasi-one-dimensional electron gas confined in a quantum well, and the absorption spectra and the induced charge density distributions are calculated based on the random-phase approximation (RPA). Here, following Ref. [19], we use the dielectric function to describe the polarization effects of semi-infinite Si substrates. The calculated results show that the redshifts of all the absorption spectra are found in both longitudinal and transverse plasmon excitations by considering the polarization effects of substrates, and the intensities of the corresponding main peaks have some variation. In particular, a significant increase in the intensities of resonant peaks appears when the direction of the external field is perpendicular to Si surfaces. In addition, the increase in the values of dielectric constants is beneficial to the redshift of plasmon peaks. Our calculations for the induced charge distributions indicate that the end (TE) mode and the central

*Corresponding author: apybyu@hnu.edu.cn

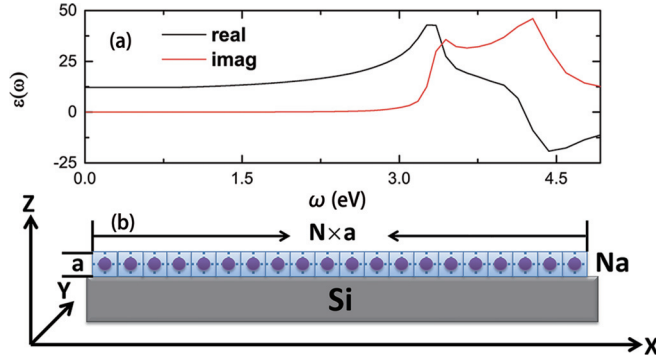


FIG. 1. (a) The real and imaginary parts of the dielectric function $\epsilon(\omega)$ for silicon as a function of the excitation frequency ω . (b) The schematic view of a Na atomic chain is mimicked by a model of a quasi-one-dimensional electron gas confined in a cubic cylinder on semi-infinite Si substrates. Here, N is the number of atoms, and a is the lattice constant.

(TC) mode [47,48] in transverse plasmon excitations arise from electron-electron interactions, which reflects the collective excitations induced by the interactions.

II. COMPUTATIONAL METHODS

We will use the standard RPA to calculate the plasmon excitations of 1D atomic chains on semiconducting substrate surfaces, and the surfaces are modeled by a semi-infinite dielectric medium with dielectric function $\epsilon(\omega) = [n(\omega) + i\kappa(\omega)]^2$, where $n(\omega)$ is the refractive index, $\kappa(\omega)$ is the extinction coefficient, and as described in Ref. [49], these empirical data take different values. In this paper, we use the data for $n(\omega)$ and $\kappa(\omega)$ for Si at room temperature provided by Green [49] to calculate the dielectric function $\epsilon(\omega)$, and the result shown in Fig. 1(a). As shown in Fig. 1(b), the 1D metal adatom chain of N Na atoms is mimicked by a model of a quasi-one-dimensional electron gas confined in a cubic cylinder with a length of $N \times a$ and a cross section of $a \times a$, where N is the number of atoms in the chain and a is the lattice constant. Each atom is situated at the center of a single lattice. In the confined quasi-one-dimensional electron-gas model, the eigenwave function can be written as

$$\Psi_n(x, y, z) = \sqrt{\frac{8}{Na^3}} \sin \frac{n_x \pi x}{Na} \sin \frac{n_y \pi y}{a} \sin \frac{n_z \pi z}{a}, \quad (1)$$

with eigenenergy $E_n = \frac{\pi^2 \hbar^2}{2m_e a^2} (\frac{n_x^2}{\mu_1 N^2} + \frac{n_y^2}{\mu_2} + \frac{n_z^2}{\mu_2})$, where $n_x = 1, 2, 3, \dots, N$, $n_y = 1, 2$, and $n_z = 1, 2$. Here, the electronic eigenfunctions with $(n_y, n_z) = (1, 1), (2, 1), (1, 2)$ are employed to mimic alkali-metal s , p_y , and p_z valence orbitals, respectively [19,20]. In the following, these eigenfunctions with the three lowest energies are considered. The ground state of this system assumes that the lowest s band is half filled, i.e., that the lowest $N/2$ [or $(N+1)/2$] levels are occupied, while the p_y and p_z bands are empty. To keep the same atomic spacing of the $N \times a$ chain as in Ref. [47], the lattice constant a is taken to be 2.89 Å. In the above equation, m_e is the mass of bare electrons, and $\mu_1 m_e, \mu_2 m_e$, and $\mu_2 m_e$ are the effective masses of the electrons in the direction of the chain (x) and directions to the chain vertical (y, z), respectively.

Here, μ_1 and μ_2 are the adjustable parameters to determine the energy differences between the levels of s electrons and between the s and p bands, so that the main plasmonic resonance frequency of the freestanding sodium chain calculated by our model is basically accordant with the one calculated by the time-dependent DFT (TDDFT; see the Appendix). According to the RPA, the induced charge density $\rho^{\text{ind}}(\mathbf{r}, \omega)$ due to a uniform external potential $V^{\text{ext}}(\mathbf{r}, \omega) = -\mathbf{r} \cdot E_0 e^{-i\omega t}$ is given by

$$\rho^{\text{ind}}(\mathbf{r}, \omega) = \int \prod(\mathbf{r}, \mathbf{r}', \omega) [V^{\text{ext}}(\mathbf{r}', \omega) + V^{\text{ind}}(\mathbf{r}', \omega)] d\mathbf{r}', \quad (2)$$

with the Lindhard function

$$\begin{aligned} \prod(\mathbf{r}, \mathbf{r}', \omega) &= 2e^2 \sum_{mn} \frac{f(E_m) - f(E_n)}{E_m - E_n - \omega - i\gamma} \\ &\times \Psi_m^*(x, y, z) \Psi_n(x, y, z) \\ &\times \Psi_n^*(x', y', z') \Psi_m(x', y', z'), \end{aligned} \quad (3)$$

where e is the unit charge, $f(E)$ is the Fermi distribution function, γ is a small damping constant that will be taken to be 0.015 unless otherwise specified, and

$$V^{\text{ind}}(\mathbf{r}, \omega) = \frac{1}{4\pi\epsilon_0} \int \rho^{\text{ind}}(\mathbf{r}', \omega) G(\mathbf{r}, \mathbf{r}') d\mathbf{r}', \quad (4)$$

where

$$\begin{aligned} G(\mathbf{r}, \mathbf{r}') &= \frac{1}{\sqrt{(x-x')^2 + (y-y')^2 + (z-z')^2}} \\ &- \frac{\epsilon(\omega) - 1}{\epsilon(\omega) + 1} \frac{1}{\sqrt{(x-x')^2 + (y-y')^2 + (z+z')^2}} \end{aligned} \quad (5)$$

is the Green's function of the system. Substituting Eqs. (2) and (3) into Eq. (4), we obtain

$$\begin{aligned} V^{\text{ind}}(\mathbf{r}, \omega) &= \frac{2e^2}{4\pi\epsilon_0} \sum_{mn} \iint d\mathbf{r}'' d\mathbf{r}' \frac{f(E_m) - f(E_n)}{E_m - E_n - \omega - i\gamma} \\ &\times \Psi_m^*(\mathbf{r}'') \Psi_n(\mathbf{r}'') \Psi_m^*(\mathbf{r}') \Psi_n(\mathbf{r}') \\ &\times G(\mathbf{r}, \mathbf{r}'') [V^{\text{ext}}(\mathbf{r}', \omega) + V^{\text{ind}}(\mathbf{r}', \omega)]. \end{aligned} \quad (6)$$

Multiplying Eq. (6) by $\Psi_{m'}^*(\mathbf{r}) \Psi_{n'}(\mathbf{r})$ and then integrating over the space, we can reach

$$\begin{aligned} \sum_{mn} [\delta_{m'n'mn} - M_{m'n'mn}(\omega)] V_{mn}^{\text{ind}}(\omega) &= \sum_{mn} M_{m'n'mn}(\omega) \\ &\times V_{mn}^{\text{ext}}(\omega), \end{aligned} \quad (7)$$

with

$$\begin{aligned} M_{m'n'mn}(\omega) &= \frac{2e^2}{4\pi\epsilon_0} \iint \sum_{mn} \frac{f(E_m) - f(E_n)}{E_m - E_n - \omega - i\gamma} \\ &\times \Psi_{m'}^*(\mathbf{r}) \Psi_{n'}(\mathbf{r}) G(\mathbf{r}, \mathbf{r}'') \\ &\times \Psi_m^*(\mathbf{r}'') \Psi_n(\mathbf{r}'') d\mathbf{r} d\mathbf{r}'', \end{aligned} \quad (8)$$

where $V_{mn}^X(\omega)$ is defined as

$$V_{mn}^X(\omega) = \int \Psi_n^*(\mathbf{r}) V^X(\mathbf{r}, \omega) \Psi_m(\mathbf{r}) d\mathbf{r}. \quad (9)$$

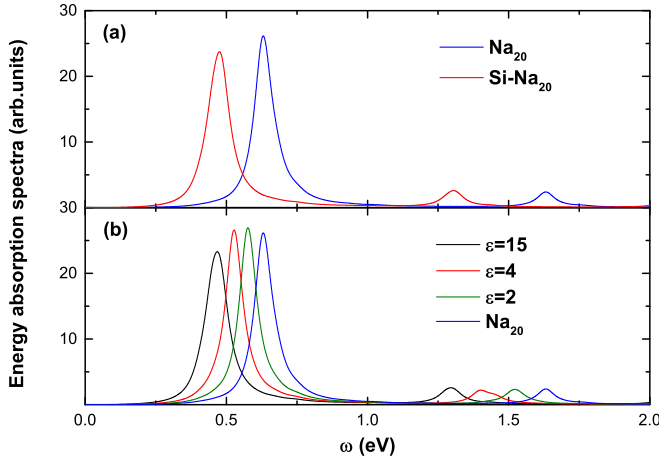


FIG. 2. The longitudinal absorption spectra of the atomic chain Na_{20} (made up of 20 Na atoms). The blue lines denote the spectra without the polarization effects of substrates, while the black, red, and green lines represent the spectra with the effects. In (a), the dielectric function of silicon $\varepsilon(\omega)$ is considered. In (b), the dielectric constants ε are 2, 4, and 15.

Finally, the induced charge density $\rho^{\text{ind}}(\mathbf{r}, \omega)$ can be calculated by the following equation:

$$\rho^{\text{ind}}(\mathbf{r}, \omega) = 2e^2 \sum_{mn} \frac{f(E_m) - f(E_n)}{E_m - E_n - \omega - i\gamma} \Psi_m^*(\mathbf{r}) \Psi_n(\mathbf{r}) \times [V_{mn}^{\text{ext}}(\omega) + V_{mn}^{\text{ind}}(\omega)], \quad (10)$$

and then the absorption spectrum function $A(\omega)$ can be obtained as [30]

$$A(\omega) = -\frac{1}{2} \omega \text{Im} \left\{ \int \rho^{\text{ind}}(\mathbf{r}, \omega) [V^{\text{ext}}(\mathbf{r}, \omega)]^* d\mathbf{r} \right\}, \quad (11)$$

with which we can get the resonance frequency ω of a plasmon peak in absorption spectra and then calculate the induced charge distribution at ω that corresponds to the peak.

III. RESULTS AND DISCUSSION

According to Eq. (11), we calculate the longitudinal and transverse absorption spectra of the atomic chain riding on Si surfaces (Si-Na_{20}) with the polarization effects of substrates. In this work, we are interested in only the plasmon excitations relative to the ground state of the system; hence, our calculation is under the condition of zero temperature [50]. In Fig. 2(a), we show the results for the longitudinal spectra obtained by applying the external fields to the chain in the x direction. For a comparison, the spectra of the same chain without the effects of substrates are also presented. The red line and the blue line in Fig. 2(a) denote the absorption spectra with and without the substrate polarization, respectively. In the spectra, a main peak appears in the blue line ($\omega = 0.6292$ eV), whereas the main peak in the red line ($\omega = 0.4752$ eV) has a redshift in comparison with the blue line. Meanwhile, the strength of the main peak at $\omega = 0.4752$ eV slightly decreases due to the substrate polarization. We can understand that the redshift and the decrease in intensity for the resonant peak are caused by the screening

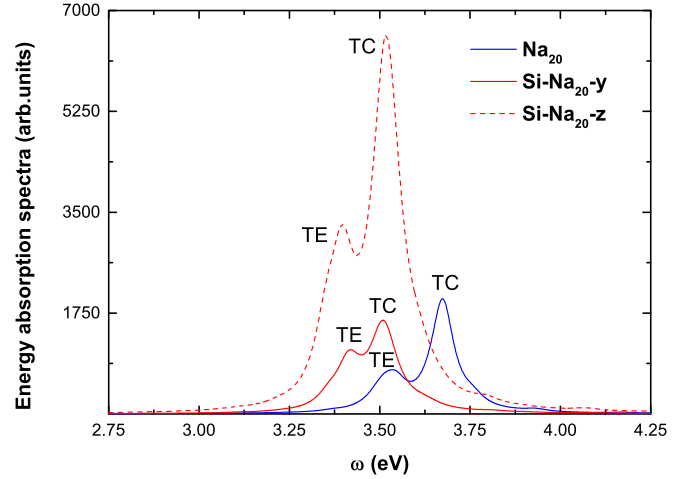


FIG. 3. The transverse absorption spectra of the atomic chain Na_{20} . The blue solid line denotes the spectra without the substrate polarization; the red solid line and the red dashed line denote the spectra without the polarization. Here, the red solid line is the spectra obtained by applying the external field in the y direction, and the red dashed line is the spectra obtained by applying the field in the z direction.

of electrons resulting from the substrate polarization in the chain. In other words, since the elastic restoring force of the system is decreased due to the screening of Coulomb interactions, the plasmon resonant peaks will suffer the redshifts in resonance energies, and the intensity of the main resonant peak is changed. In our recent work, the TDDFT calculations of Au atomic chains showed that the resonance energies of plasmon excitations are considerably reduced by d -electron screening [40]. In fact, our further investigations show that with the increase of dielectric constants the redshifts of the main peaks are enhanced, and the intensities of the peaks have some variation, but it is not monotonic. This conclusion can be illustrated by Fig. 2(b), in which we compare the absorption spectra of the Na_{20} chain riding on three different substrates with that of the freestanding Na_{20} chain, and their dielectric constants are 2, 4, and 15.

Next, we will investigate the polarization effects of substrates on the transverse-mode plasmon excitations. Figure 3 shows the transverse absorption spectra of the same chains, which are obtained by applying the external fields in the y and z directions. As expected, for the chains both with and without the polarization effects of substrates two resonant peaks appear in the spectra, which correspond to the transverse TE and TC modes of plasmon excitations [47]. Compared with the two peaks of the freestanding chain (Na_{20}) at $\omega = 3.532$ eV and $\omega = 3.67$ eV, in the chains with the polarization effects of substrates one can observe the redshifts of the plasmon peaks for both the y -direction excitation (Si-Na_{20-y}) and the z -direction excitation (Si-Na_{20-z}). Meanwhile, in the y -direction excitation, the intensity of the low-energy peak (corresponding to the TE mode at $\omega = 3.418$ eV) is considerably enhanced, while the high-energy peak (corresponding to the TC mode at $\omega = 3.505$ eV) is somewhat suppressed. However, in the z -direction excitation, the intensities of the two peaks at $\omega = 3.394$ eV and $\omega = 3.514$ eV are all

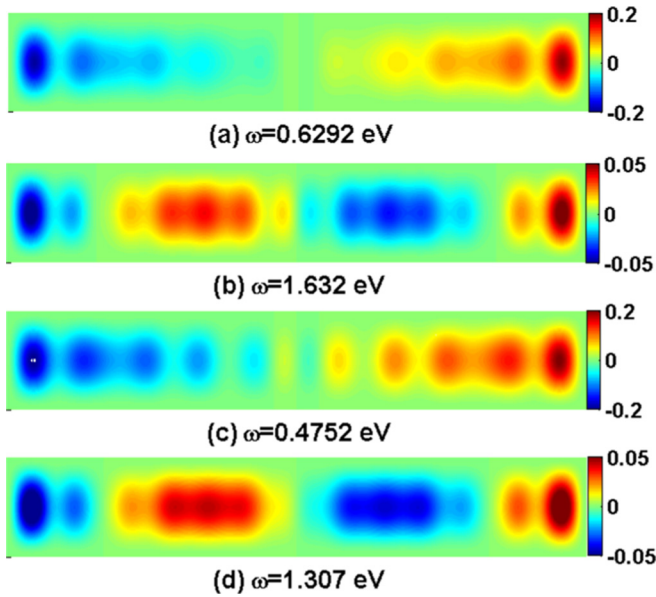


FIG. 4. The induced charge distributions for the longitudinal resonances corresponding to the frequencies of the main peaks and the subpeaks in Fig. 2(a). In (a) and (b) the substrate polarization is not taken into account, and in (c) and (d) the substrate polarization is taken into account.

enhanced greatly. This is because in the z -direction excitation, in addition to the polarization of substrates caused by the induced charges in the chains, the substrates are polarized by the external field perpendicular to substrate surfaces, produce an additional field in the same direction as the external field, and hence effectively enhance the external field, while in the x - and y -direction excitations, there is only the polarization caused by the induced charges in the chains.

To further illustrate the polarization effects of substrates on plasmon excitations, we calculate the induced charge distributions by using the frequency ω of each plasmon resonant peak. Because the absorption spectrum $A(\omega)$ is related to only the imaginary part of the induced charge density $\rho^{\text{ind}}(\mathbf{r}, \omega)$ [see Eq. (11)], here, only the imaginary part of the induced charge distributions will be presented. Figure 4 shows the induced charge distributions of the main peaks and the subpeaks for longitudinal resonances in the atomic chains Na_{20} with and without the polarization effects of substrates, where the induced charges are in the plane $z = 0$ Å. The charge distributions of the main longitudinal resonances in the chains without and with substrate effects are shown in Figs. 4(a) and 4(c), respectively. The distribution of induced charges in Fig. 4(a) is a typical dipolar plasmon mode of longitudinal resonances for freestanding Na atomic chains. The induced charge oscillations are antisymmetric with respect to the central line perpendicular to the direction of the external field, and its amplitude reaches the maximum in the end. Due to the polarization effects of substrates, in Fig. 4(c) the strength of the oscillating charges in the central area slightly increases in comparison with Fig. 4(a). For the induced charge distributions of small longitudinal plasmon resonant peaks, Figs. 4(b) and 4(d) show charge oscillations along the chain lengths, and local polarizations significantly appear in the chain.

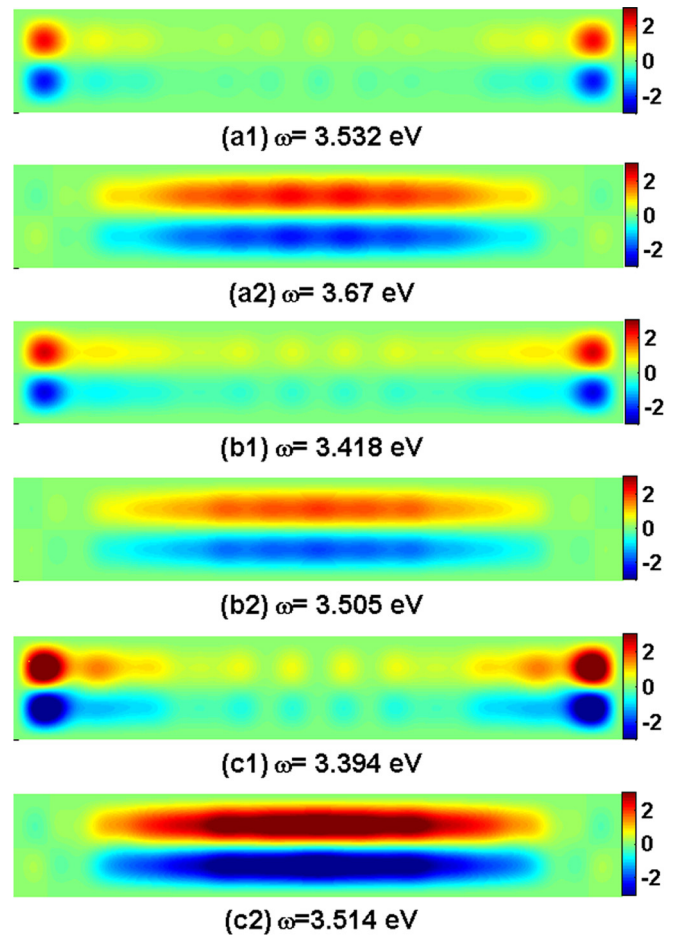


FIG. 5. The induced charge distributions for the transverse resonances corresponding to the frequencies of the main peaks and the subpeaks in Fig. 3. In (a1) and (a2) the substrate polarization is not taken into account, and in (b1), (b2), (c1), and (c2) the substrate polarization is taken into account. Here, in (a1), (a2), (b1), and (b2) the external fields are applied along the y axis; in (c1) and (c2) they are perpendicular to the Si surfaces along the z axis.

Figure 5 shows the induced charge distributions at the transverse resonant peaks in the chains. One can find that the charge distributions in the chains with the substrate effects still correspond to the TE and TC modes [47], in which the electronic oscillating regions are mainly around the end and center of the chains, respectively. In Figs. 5(a1) and 5(a2), we present the charge distributions induced by the field in the y direction for the chains without the polarization effects of substrates. Due to the polarization effects of substrates, in Fig. 5(b1) the oscillation strength of the induced charges has an enhancement in comparison with Fig. 5(a1), whereas in Fig. 5(b2) the oscillation strength is slightly reduced in comparison with Fig. 5(a2), but not obviously. When the external field is applied along the z axis, the oscillation strengths of both the TE and TC modes with the polarization effects of substrates [Figs. 5(c1) and 5(c2)] are much stronger than the ones without the polarization effects of substrates [Figs. 5(a1) and 5(a2)]. These results are in good agreement with the analysis of the above absorption spectra. We can conclude that

the polarization effects of substrates do not disrupt the charge oscillations of the plasmon modes but affect their intensities.

Finally, we want to discuss the formation mechanism of the TE and TC modes which appear in the chains excited by the field in the transverse directions. Obviously, the origin of the two transverse modes is related to the s - p interband transition of electrons, while the longitudinal mode is related to the intraband transition of s electrons. This can be inferred from Eqs. (7), (9), and (10) because the transition matrix of the transverse field is zero between different electron states in the s band of the chains, while the transition matrix of the longitudinal field is zero between the s and p bands in our one-dimensional electron-gas model. It needs to be pointed out that, generally, the transition matrix of the longitudinal field is not zero between s and p bands in first-principles calculations, so longitudinal excitation also has high-energy plasmon excitations from the s - p interband transition, whereas we discuss only the low-energy plasmon excitations in the longitudinal mode. On the other hand, we find it is also true for the first-principles calculations that the transverse plasmon excitations come from only the s - p interband transition of electrons. This may be understood as follows. The orthonormalized wave functions of electrons in the s band of the chains can be written as $\psi_{sk}(x, y, z) = \sum_l C_{skl} \phi_s(x - x_l, y, z)$, where $\sum_l C_{skl}^* C_{sk'l} = \delta_{kk'}$,

$\phi_s(x - x_l, y, z)$ is the Wannier function and $\int \phi_s^*(x - x_l, y, z) \phi_s(x - x_{l'}, y, z) dx \approx \delta_{ll'}$, $\int \phi_s^*(x, y, z) \phi_s(x, y, z) dx \approx \delta_{kk'}$ so that $\int \psi_{sk}^*(x, y, z) y \psi_{sk'}(x, y, z) dx dy dz \approx \delta_{kk'}$, $\int \psi_{sk}^*(x, y, z) y \psi_{sk}(x, y, z) dx dy dz \approx \delta_{kk'}$ and $\int \psi_{sk}^*(x, y, z) z \psi_{sk'}(x, y, z) dx dy dz \approx \delta_{kk'}$, $\int \psi_{sk}^*(x, y, z) z \psi_{sk}(x, y, z) dx dy dz \approx \delta_{kk'}$. In addition, according to Eqs. (1) and (9), the interband transition is only between transverse states (1,1) and (2,1) of the y -direction excitation or between (1,1) and (1,2) of the z -direction excitation. So what makes the two peaks appear in the transverse excitations? In order to simplify the question, the following discussions are about the freestanding chain Na_{20} . In Fig. 6(a), we present the y -direction dipole response spectrum in the chain of the noninteracting electrons, which is obtained by setting $V^{\text{ind}}(\mathbf{r}, \omega) = 0$, and as expected, only one peak appears at $\omega = 1.744$ eV. Figure 6(b) shows the induced charge distribution of the chain corresponding to this peak, and one can find that the distribution does not completely have the characteristics of the TE and TC modes. Figures 6(c) and 6(d) show the charge distributions caused by only the induced inner potential $V^{\text{ind}}(\mathbf{r}, \omega)$, which is excited by the two resonant frequencies of the TE and TC modes. One can observe that the oscillating charges caused by $V^{\text{ind}}(\mathbf{r}, \omega)$ display the features of the TE mode and the TC mode. However, in Fig. 6(b) the oscillation mode caused by only $V^{\text{ext}}(\mathbf{r}, \omega)$ spreads in the entire chain. Therefore, it can be concluded that the charge oscillations of the TE and TC modes are mainly caused by electron-electron interactions, which reflects the collective excitations induced by the interactions.

IV. CONCLUSIONS

The polarization effects of substrates are essential for theoretical investigations on the electronic excitations of substrate-chain systems, and that is an unavoidable topic

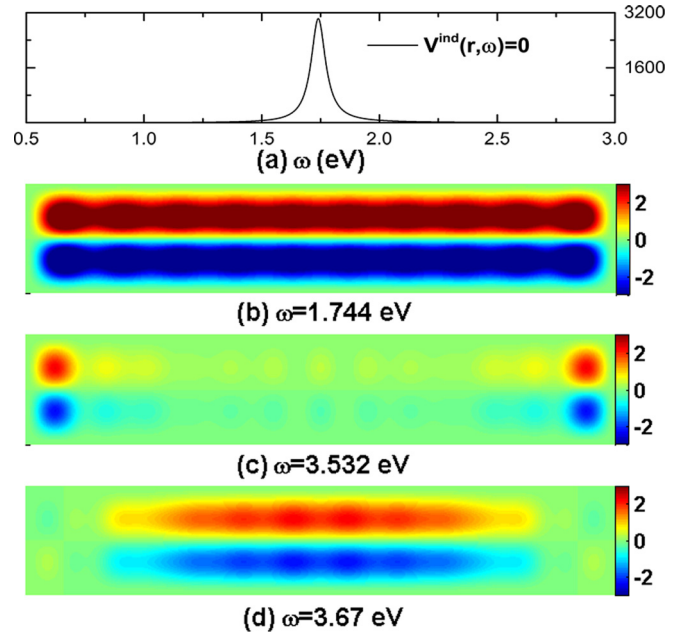


FIG. 6. (a) The y -direction dipole response spectrum of the atomic chain Na_{20} without electron-electron interactions and (b) the corresponding induced charge distribution for the resonance frequency. (c) and (d) The charge distributions for the two resonance frequencies of the TE and TC modes excited in the y direction shown in Fig. 3; here, only the induced inner potential $V^{\text{ind}}(\mathbf{r}, \omega)$ is taken into account.

for prospective applications of nanoelectronic devices. Based on the random-phase approximation and a free-electron-gas model taking a semi-infinite dielectric medium as the substrate, we have systematically investigated the plasmon excitations of a small Na chain riding on Si surfaces. The primary conclusions of the paper are as follows:

(1) Due to the polarization effects of Si substrates, redshifts of plasmon peaks have been found in both longitudinal and transverse absorption spectra, and the intensities of the main

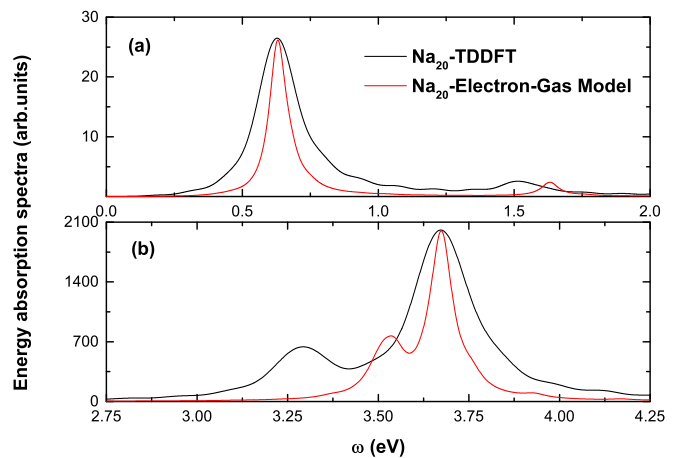


FIG. 7. (a) and (b) are the longitudinal and transverse absorption spectra of the freestanding Na_{20} chain, respectively. Here, the red lines represent the spectra calculated by the electron-gas model, and the black lines represent the ones calculated by the TDDFT.

peaks on plasmon resonances have some variation; in particular, the intensity gets a very large enhancement when the direction of the external field is perpendicular to Si surfaces.

(2) The increase in the values of dielectric constants is in favor of the redshifts of plasmon resonant peaks, and the strengths of the peaks have some variation, but it is not monotonic.

(3) When the direction of the applied external field is perpendicular to substrate surfaces, the oscillation strength of induced charges of plasmon resonances is greatly affected by the polarization effects of the substrates, while in other cases the influences are relatively small.

(4) Meanwhile, studies on the formation mechanism of the end mode and the central mode tell us that the two modes are caused by electron-electron interactions, which reflects the collection excitations induced by the interactions.

ACKNOWLEDGMENTS

This work is financially supported by the National Natural Science Foundation of China (Grants No. 10774041 and No. 11675051), the Key Scientific Research Platforms and Projects in Guangdong Universities (Grant No. 2018KZDXM046), and the Natural Science Foun-

dation of Guangdong Province in China (Grant No. 2019A1515011132).

APPENDIX

As mentioned in Sec. II, we employed the confined quasi-one-dimensional electron-gas model to mimic the Na atomic chain. In order to make the eigenwave function equation (1) and the corresponding eigenenergies sufficient approximations to the electron structure of the chain of Na atoms, μ_1 and μ_2 are set to be adjustable parameters. We adjust the energy difference between the highest occupied energy level and the lowest unoccupied level in the s band $\frac{121}{400} \frac{\pi^2 \hbar^2}{2\mu_1 m_e a^2}$ to 0.13 eV and the energy difference between the s and p bands $\frac{3\pi^2 \hbar^2}{2\mu_2 m_e a^2}$ to 1.74 eV, so that the absorption spectra of the freestanding Na₂₀ chain calculated by the electron-gas model are basically consistent with the one calculated by the TDDFT, as shown in Fig. 7. Here, Figs. 7(a) and 7(b) show, respectively, the longitudinal and transverse absorption spectra of the freestanding Na₂₀ chain calculated by using the electron-gas model and the TDDFT method. All the TDDFT calculations are based on the real-time TDDFT code in the OCTOPUS package [51,52], and the details of the calculations can be found in Ref. [40].

-
- [1] H. Shin and S. Fan, *Phys. Rev. Lett.* **96**, 073907 (2006).
- [2] X. Fan, G. P. Wang, J. C. W. Lee, and C. T. Chan, *Phys. Rev. Lett.* **97**, 073901 (2006).
- [3] V. M. Shalaev, *Nat. Photonics* **1**, 41 (2007).
- [4] S. Kim, J. Jin, Y. J. Kim, I. Y. Park, Y. Kim, and S. W. Kim, *Nature (London)* **453**, 757 (2008).
- [5] J. M. Fitzgerald, S. Azadi, and V. Giannini, *Phys. Rev. B* **95**, 235414 (2017).
- [6] P. Christopher, D. B. Ingram, and S. Linic, *J. Phys. Chem. C* **114**, 9173 (2010).
- [7] S. Linic, U. Aslam, C. Boerigter, and M. Morabito, *Nat. Mater.* **14**, 567 (2015).
- [8] H. Baida, D. Mongin, D. Christofilos, G. Bachelier, A. Crut, P. Maioli, N. Del Fatti, and F. Vallee, *Phys. Rev. Lett.* **107**, 057402 (2011).
- [9] M. Kauranen and A. V. Zayats, *Nat. Photonics* **6**, 737 (2012).
- [10] E. Hutter and J. H. Fendler, *Adv. Mater.* **16**, 1685 (2004).
- [11] F. Edler, I. Miccoli, J. P. Stockmann, H. Pfnur, C. Braun, S. Neufeld, S. Sanna, W. G. Schmidt, and C. Tegenkamp, *Phys. Rev. B* **95**, 125409 (2017).
- [12] T. Aruga, H. Tochihara, and Y. Murata, *Phys. Rev. Lett.* **53**, 372 (1984).
- [13] D. M. Eigler and E. K. Schweizer, *Nature (London)* **344**, 524 (1990).
- [14] N. Nilius, T. M. Wallis, and W. Ho, *Science* **297**, 1853 (2002).
- [15] G. V. Nazin, X. H. Qiu, and W. Ho, *Phys. Rev. Lett.* **90**, 216110 (2003).
- [16] T. Lichtenstein, Z. Mamiyev, C. Braun, S. Sanna, W. G. Schmidt, C. Tegenkamp, and H. Pfnur, *Phys. Rev. B* **97**, 165421 (2018).
- [17] N. Oncel, *J. Phys.: Condens. Matter* **20**, 393001 (2008).
- [18] S. Sanna, T. Lichtenstein, Z. Mamiyev, C. Tegenkamp, and H. Pfnur, *J. Phys. Chem. C* **122**, 25580 (2018).
- [19] M. Tsukada, H. Ishida, and N. Shima, *Phys. Rev. Lett.* **53**, 376 (1984).
- [20] H. Ishida, N. Shima, and M. Tsukada, *Phys. Rev. B* **32**, 6246 (1985).
- [21] T. Lichtenstein, J. Aulbach, J. Schafer, R. Claessen, C. Tegenkamp, and H. Pfnur, *Phys. Rev. B* **93**, 161408(R) (2016).
- [22] R. K. Moudgil, V. Garg, and K. N. Pathak, *J. Phys.: Condens. Matter* **22**, 135003 (2010).
- [23] A. Liebsch, *Phys. Rev. Lett.* **71**, 145 (1993).
- [24] E. H. Hwang and S. Das Sarma, *Phys. Rev. B* **75**, 205418 (2007).
- [25] J. M. McMahon, S. K. Gray, and G. C. Schatz, *Phys. Rev. Lett.* **103**, 097403 (2009).
- [26] K. Y. Lian, P. Salek, M. Jin, and D. Ding, *J. Chem. Phys.* **130**, 174701 (2009).
- [27] B. J. Wang, Y. Xu, and S. H. Ke, *J. Chem. Phys.* **137**, 054101 (2012).
- [28] G. Piccini, R. W. A. Havenith, R. Broer, and M. Stener, *J. Phys. Chem. C* **117**, 17196 (2013).
- [29] F. Ding, E. B. Guidez, C. M. Aikens, and X. Li, *J. Chem. Phys.* **140**, 244705 (2014).
- [30] Y. Wang and Y. B. Yu, *Int. J. Mod. Phys. B* **31**, 1750233 (2017).
- [31] K. M. Conley, N. Nayyar, T. P. Rossi, M. Kuisma, V. Turkowski, M. J. Puska, and T. S. Rahman, *ACS Nano* **13**, 5344 (2019).
- [32] R. D. Senanayake, D. B. Lingerfelt, G. U. Kuda-Singappulige, X. Li, and C. M. Aikens, *J. Phys. Chem. C* **123**, 14734 (2019).
- [33] N. Nayyar, V. Turkowski, and T. S. Rahman, *Phys. Rev. Lett.* **109**, 157404 (2012).
- [34] S. Gao and Z. Yuan, *Phys. Rev. B* **72**, 121406(R) (2005).
- [35] T. Dong, X. Ma, and R. Mittra, *Appl. Phys. Lett.* **101**, 233111 (2012).
- [36] A. O. Govorov and H. Zhang, *J. Phys. Chem. C* **119**, 6181 (2015).

- [37] H. T. Smith, T. E. Karam, L. H. Haber, and K. Lopata, *J. Phys. Chem. C* **121**, 16932 (2017).
- [38] A. Castro, M. A. L. Marques, A. H. Romero, M. J. T. Oliveira, and A. Rubio, *J. Chem. Phys.* **129**, 144110 (2008).
- [39] M. H. Khodabandeh, N. Asadi-Aghbolaghi, and Z. Jamshidi, *J. Phys. Chem. C* **123**, 9331 (2019).
- [40] J. Chen, L. Q. Lai, X. Yang, Q. H. Liu, and Y. B. Yu, *Phys. Rev. B* **101**, 085421 (2020).
- [41] L. Yan, M. Guan, and S. Meng, *Nanoscale* **10**, 8600 (2018).
- [42] T. Nagao, S. Yaginuma, T. Inaoka, T. Sakurai, and D. Jeon, *J. Phys. Soc. Jpn.* **76**, 114714 (2007).
- [43] C. Liu, T. Inaoka, S. Yaginuma, T. Nakayama, M. Aono, and T. Nagao, *Phys. Rev. B* **77**, 205415 (2008).
- [44] U. Krieg, Y. Zhang, C. Tegenkamp, and H. Pfnur, *New J. Phys.* **16**, 043007 (2014).
- [45] F. Hotzel, K. Seino, C. Huck, O. Skibbe, F. Bechstedt, and A. Pucci, *Nano Lett.* **15**, 4155 (2015).
- [46] Z. Mamiyev and H. Pfnur, *Phys. Rev. B* **102**, 075438 (2020).
- [47] J. Yan, Z. Yuan, and S. Gao, *Phys. Rev. Lett.* **98**, 216602 (2007).
- [48] J. Yan and S. Gao, *Phys. Rev. B* **78**, 235413 (2008).
- [49] M. A. Green, *Sol. Energy Mater. Sol. Cells* **92**, 1305 (2008).
- [50] Since the dielectric function $\varepsilon(\omega)$ for Si at zero temperature is not available, the data at room temperature in Ref. [49] are used, but we believe this choice will not affect the results qualitatively.
- [51] M. A. L. Marques, A. Castro, G. F. Bertsch, and A. Rubio, *Comput. Phys. Commun.* **151**, 60 (2003).
- [52] A. Castro, H. Appel, M. Oliveira, C. A. Rozzi, X. Andrade, F. Lorenzen, M. A. L. Marques, E. K. U. Gross, and A. Rubio, *Phys. Status Solidi B* **243**, 2465 (2006).